# Quantitative Evaluation of the Thickness of the Available Manipulation Volume Inside the Knee Joint Capsule for Minimally Invasive Robotic Unicondylar Knee Arthroplasty

Manuela Eugster , *Student Member, IEEE*, Esther I. Zoller , *Student Member, IEEE*, Philipp Krenn, Sandra Blache, Niklaus F. Friederich , Magdalena Müller-Gerbl , Philippe C. Cattin , *Member, IEEE*, and Georg Rauter , *Member, IEEE*

*Abstract*—*Objective:* Developing robotic tools that introduce substantial changes in the surgical workflow is challenging because quantitative requirements are missing. Experiments on cadavers can provide valuable information to derive workspace requirements, tool size, and surgical workflow. This work aimed to quantify the volume inside the knee joint available for manipulation of minimally invasive robotic surgical tools. In particular, we aim to develop a novel procedure for minimally invasive unicompartmental knee arthroplasty (UKA) using a robotic laser-cutting tool. *Methods:* Contrast solution was injected into nine cadaveric knees and computed tomography scans were performed to evaluate the tool manipulation volume inside the knee joints. The volume and distribution of the contrast solution inside the knee joints were analyzed with respect to the femur, tibia, and the anatomical locations that need to be reached by a laser-cutting tool to perform bone resection for a standard UKA implant. *Results:* Quantitative information was determined about the tool manipulation volume inside these nine knee joints and its distribution around the cutting lines required for a standard implant. *Conclusion:* Based on the volume distribution, we could suggest a possible workflow for minimally invasive UKA, which provides a large manipulation volume, and deducted that for the proposed workflow, an instrument with a thickness of 5-8 mm should be feasible. *Significance:* We present quantitative information on the three-dimensional distribution of the maximally available volume inside the knee joint. Such quantitative information lays the basis for developing surgical tools that introduce substantial changes in the surgical workflow.

*Index Terms*—Knee arthroplasty, knee joint volume, minimally invasive knee surgery, surgical robotics.

## I. INTRODUCTION

KNEE arthroplasty is a surgical intervention for the treatment of advanced osteoarthritis of the knee. In this procedure, the damaged bone and cartilage are replaced with implants. Different forms of knee arthroplasty, such as total knee arthroplasty (TKA) or unicompartmental knee arthroplasty (UKA) exist. UKA is a less invasive alternative to TKA for cases where only one, i.e., the medial or lateral, knee compartment, is affected. The advantages of UKA compared to TKA include reduced blood loss [1], [2], lower infection rate [3], less postoperative pain [4], faster recovery [1], better preservation of range-of-motion [5], better function [6], and lower cost [7].

However, compared to TKA, UKA is less resistant to component malalignment [8] and to achieve long-term success of a unicondylar knee implant, correct alignment of the implant components is crucial [9]. Poor implant positioning in UKA may lead to early implant wear, poor functional results, and a higher revision rate [10], [11]. Besides, performing UKA with a smaller incision (less invasively) may reduce visible anatomical landmarks compared to conventional UKA. This would make the intraoperative orientation and proper positioning of the components even more difficult [12].

The use of robots could help overcome some of UKA's technical difficulties, whereas maintaining its benefits compared to TKA. For example, robotic assistance has the potential to facilitate more accurate implant component positioning [13]–[15]. Currently, there are two systems for robot-assisted UKA that both are FDA approved and CE-marked: the Mako (Stryker, Mahwah, NJ) and the Navio (Smith & Newphew, Memphis, TN) [16]. These two robotic systems have shown to improve implant placement accuracy, tibial alignment, and ligament

balance in UKA [17]. Improved tibial alignment has been shown to increase implant survival and decrease the need for revision surgery [18]. These results show that robotic surgery can improve the precision and accuracy of UKA, resulting in implants being placed more in accordance with preoperative planning [19].

However, the aforementioned robotic systems for UKA are equally or even more invasive than conventional, non-robotic UKA. This could be due to the need to introduce additional devices for fixation during surgery, exposure of anatomical landmarks for registration, and the required space for the robotic equipment [19]. It is known from other surgery areas that less invasive procedures result in less collateral damage to healthy tissue and faster patient recovery, [20], [21].

Therefore, we are currently developing a robotic device for a novel technique for minimally invasive UKA based on laser osteotomy, facilitating highly accurate implant placement according to preoperative planning [22]. Laser osteotomy offers a low contact force alternative to cutting bone with conventional mechanical tools [23]. In addition, cutting with a laser has been shown to result in faster bone healing, higher cutting precision, improved cutting-depth control [24], and increased freedom in the cutting geometry compared to cutting with mechanical tools [25]. Our device will consist of a flexible robotic endoscope inserted into the knee joint through a small incision (Fig. 1). The cutting laser will be guided through the endoscope to the tip by an optical fiber. The robotic endoscope's tip will consist of a stand-alone miniature parallel robot housing the laser optics that redirect the laser beam toward the bone surface. The laser optics will have a long depth of focus to enable the realization of especially deep bone cuts. A microelectromechanical systems mirror integrated into the laser optics will enable angular deflections of the laser. The miniature parallel robot will need at least three planar active degrees of freedom (DoFs) to position the laser for cutting on a large scale. This miniature parallel robot is currently being developed and has two legs that attach to the bone to improve the stabilization and accuracy of the laser cutting process and to allow expanding the workspace of the device [26], [27]. The leg's position relative to the bone will be fixed based on a non-invasive concept such as e.g., suction cups or balloon catheters.

The development of such a robotic tool for minimally invasive surgery poses many challenges. One of the main challenges is the lack of a formal design methodology. There is limited literature documenting requirements for robotic manipulation inside a living human body, such as the forces required to manipulate a robotic tool or the available workspace within human cavities [28]. From a medical point of view, minimally invasive tools are better the smaller they are. However, from an engineering point of view, the complexity of the device and the costs for development and manufacturing are inversely proportional to the instrument size. Therefore, knowing the maximal feasible instrument size is essential for its development.

In case an existing surgical technique is robotized, it could be possible to develop robotic instruments without the explicit knowledge of the quantitative characteristics of the target anatomy by developing instruments similar to existing surgical
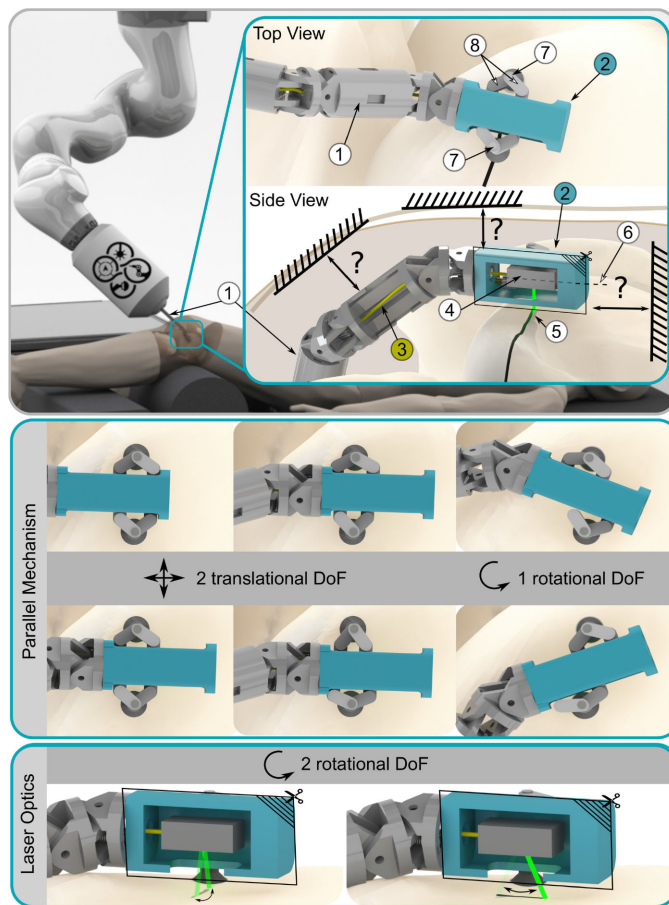


Fig. 1. Illustration of the novel device for minimally invasive unicompartmental knee arthroplasty: A robotic endoscope ① is inserted into the knee joint. The cutting laser is guided through the endoscope to the endoscope tip ② by an optical fiber ③. The laser optics ④ redirect the laser beam ⑤, which then exits the endoscope tip perpendicular to its longitudinal axis ⑥ towards the bone surface below the robot. The endoscope tip has two legs ⑦ whose positions are fixed relative to the bone surface. A parallel mechanism ⑧ allows to move the laser optics in two translational and one rotational degrees of freedom (DoFs), whereas the laser optics will allow to deflect the laser in additional two rotational DoFs. The available manipulation volume for the robotic device inside in the knee joint is unknown.

tools or robotizing existing surgical tools, e.g., robotized endoscopes to facilitate endoscope manipulation (e.g., [29] or [30]). Another option is to analyze the surgical procedure of interest, e.g., by collecting data such as the instrument motion (e.g., [31]) or interaction forces (e.g., [32] or [33]) during the procedure. However, in our case, since a novel surgical workflow is being developed, the analysis of the characteristics of the target anatomy is essential for the derivation of a possible workflow and the definition of the corresponding instrument requirements.

We have conducted a pilot study to estimate contact forces that arise while manipulating a surgical tool inside the knee joint [34]. However, information on the volume available for manipulating surgical tools inside the knee joint is lacking. The size of standard orthopedic tools used in arthroscopy may be used as a reference, but the proposed laser cutting concept requires our device to reach different locations than standard UKA tools. Only very limited quantitative information on the

TABLE I
KNEES AND RESPECTIVE BODY DONORS USED FOR THIS STUDY

| No. | Gender | Age at death in years | Body height | Knee side | Measured knee flexion angle |
|-----|--------|-----------------------|-------------|-----------|------------------------------|
| 1 | female | 84 | 151 cm | right | 56° |
| 2 | male | 91 | 175 cm | right | 47° |
| 3 | female | 98 | 154 cm | right | 51° |
| 4 | female | 80 | 160 cm | right | 52° |
| 5 | male | 88 | 173 cm | right | 53° |
| 6 | female | 87 | 154 cm | left | 45° |
| 7 | female | 100 | 152 cm | left | 55° |
| 8 | female | 94 | 170 cm | left | 59° |
| 9 | male | 77 | 177 cm | left | 48° |
| mean | - | 89 | 163 cm | - | 52° |
| std | - | 8 | 11 cm | - | 5° |

volume inside the knee joint capsule is available. McNair *et al.* [35] injected 60 ml of fluid into the knee joint capsule of their participants and assessed how much fluid was located in different transversal magnetic resonance imaging (MRI) slices before and after exercise. Whereas this gives a first idea of the joint volume distribution along the leg axis, it does not provide any information about the maximum available volume in the knee joint capsule or how it is distributed in the transverse plane. To the best of our knowledge, no data is published on the volume available for manipulation of a robotic instrument inside the knee joint through a minimally invasive incision.

Therefore, we aimed to evaluate the volume inside the knee joint capsule available for manipulation of surgical instruments, e.g., the tip of a flexible robotic endoscope. This is an essential measure for the successful development of surgical instruments, new surgical techniques, or implant designs that optimally use the volume available for instrument manipulation. Specifically, knowledge about the available volume of the knee joint capsule allows defining the maximum feasible size of surgical instruments and the anatomical sites that can be reached inside the knee joint with a given instrument for minimally invasive procedures. Based on this study's findings, we propose a surgical workflow for minimally invasive bone cutting for a standard UKA implant with a novel robotic laser osteotome. However, the findings might also facilitate the development of novel robotic tools for other minimally invasive procedures in the knee joint, such as minimally invasive cartilage replacement surgery.

## II. EVALUATION OF THE KNEE JOINT VOLUME

### A. Experimental Setup and Procedure

The volume of the knee joint capsule was examined in nine Thiel-embalmed knee specimens. Thiel soft-fix embalmed bodies were used because in contrast to Formalin embalming, Thiel embalming retains the flexibility of the tissue [36]. Details on the knees used for this study and the respective body donors are listed in Table I. This study has been approved by the Ethics Committee of Northwest/Central Switzerland, Basel (No. 2018-00157, date of approval: 16.02.2018).

Each body was positioned on the bed of a computed tomography (CT) scanner (Siemens Somatom Emotion 16 Slicer,
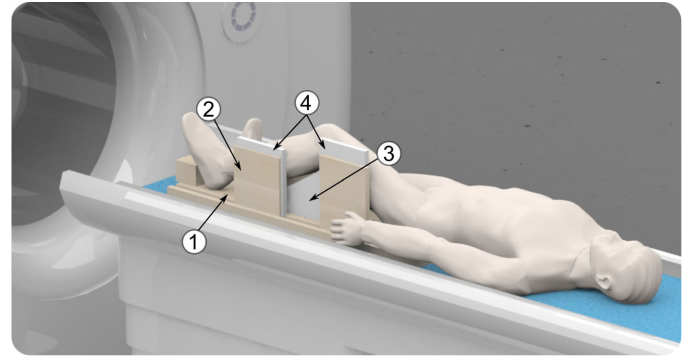


Fig. 2. Experimental setup: The body was placed on the bed of the computed tomography (CT) scanner. A custom-built wooden construction, consisting of a base plate ① and side plates ②, and a styrofoam wedge ③ were used to position the knee joint in the desired position and flexion angle. To avoid potential artefacts of the wooden side plates in the CT image, styrofoam plates ④ were placed between the side plates and the leg.

Siemens Medical Solutions USA, Inc., PA, USA) and both knees were inspected for any indications of surgical interventions or injuries. Based on these observations, the healthier knee was selected and it was ensured that none of the chosen knees had an implant. A styrofoam wedge was placed beneath the knee joint. We adjusted the knee flexion angle to approximately 50° using a goniometer. For lateral stabilization of the leg a custom-built wooden construction was used. To avoid artifacts in the CT scan, styrofoam plates were placed between the wooden side plates and the knee joint. If necessary, ropes were installed to fix the legs on the wooden construction. To stabilize the foot, additional wooden plates or styrofoam wedges were placed on the base plate. A schematic visualization of the experimental setup is presented in Fig. 2. The CT images were acquired with an isotropic spatial resolution of approximately 0.3 mm. At the beginning of each CT scan, the flexion angle was checked in a lateral view, because the exact adjustment of the knee flexion angle using only a goniometer is not possible. The flexion angle was measured between the line from the center of the visible knee condyle to the center of the hip joint and the line from the center of the visible knee condyle to the upper ankle joint center. If the measured knee flexion angle was not between 45° and 60°, the knee was repositioned and the procedure repeated. This range was selected because the relevant volume for knee surgery was expected to be the largest in this range. The resulting knee flexion angles are listed in Table I.

An iodine-based contrast solution was injected into the joint capsule to measure the volume of the knee joint capsule. We used a lateral soft spot for injection into the knee joint and inserted an indwelling venous cannula, Vasofix Safety 18G × 1 3/4 (B. Braun Melsungen AG, Melsungen, Germany). The used contrast solution was Iopamiro 300 by Bracco (Bracco, MN, USA), an iopamidolum with an iodine content of 300 mg/ml, in a 1:1 solution with natrium chloride (NaCl) 9 mg/ml by Fresenius (Fresenius SE and Co. KGaA, Bad Homburg, Germany). To limit the injection pressure, we used an injectomat Agilia (Fresenius Kabi AG, Bad Homburg, Germany). The device was set to
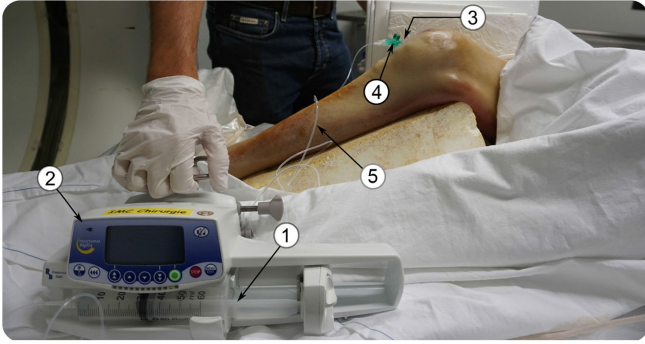
Fig. 3. Preparation of the knee for injection of the iodine-based contrast solution: The solution was filled into a syringe ①, which was mounted in the injectomat ②. The knee was punctured at a lateral soft spot ③ using an indwelling venous cannula ④. The cannula was connected to the syringe by a standard connection tube ⑤.

provide a continuous injection of 200 ml/h with a pressure alarm when exceeding 300 mmHg. A 50 ml Luer Lock syringe (B. Braun Melsungen AG, Melsungen, Germany) with contrast solution was clamped into the injectomat and connected to the cannula by a connection tube. The connection tube was filled with contrast solution prior to connection to the cannula, thereby reducing the amount of air entering the knee joint (Fig. 3).

During the injection process, periodic CT scans were performed to determine at what point the injected contrast solution started to leak out of the joint capsule and into the surrounding tissue. The injection was terminated at 95 ml for one knee, and at 115 ml for the other eight knees, because the injected contrast solution started to infiltrate adjacent tissue.

### B. Data Processing and Analysis

After the image acquisition, the CT data were evaluated in two further steps: data processing and data analysis (Fig. 4).

All nine knees were segmented manually using the software 3D Slicer 4.8.0 [37], [38]. For this purpose labels were added to the CT voxels, indicating if the voxel represented contrast solution, air, femoral bone, tibial bone, patella, fibula, or other tissue. The segmentation was carried out by an engineer and a laboratory technician from the Anatomical Institute and reviewed by an orthopedic surgeon and an anatomy specialist.

The label maps were imported in Matlab (Version 2019b, The MathWorks, Inc., MA, USA) and the labels for contrast solution and air were combined, because both represent the available tool manipulation volume inside the knee joint capsule. The corresponding three-dimensional vertices were generated for the available tool manipulation volume and each bone structure. For each of these sets of vertices, the volume enclosing surface was created in the form of a triangular mesh using the built-in Matlab function "*boundary*" with a shrink factor of 1, which resulted in a compact boundary around the vertices. The surface meshes consisted of a number of faces in the order of magnitude of $10^5$.

Image analysis aimed to calculate the thickness of the manipulation volume in the knee joint orthogonal to the bone surface. In the following, the data analysis procedure is described for the
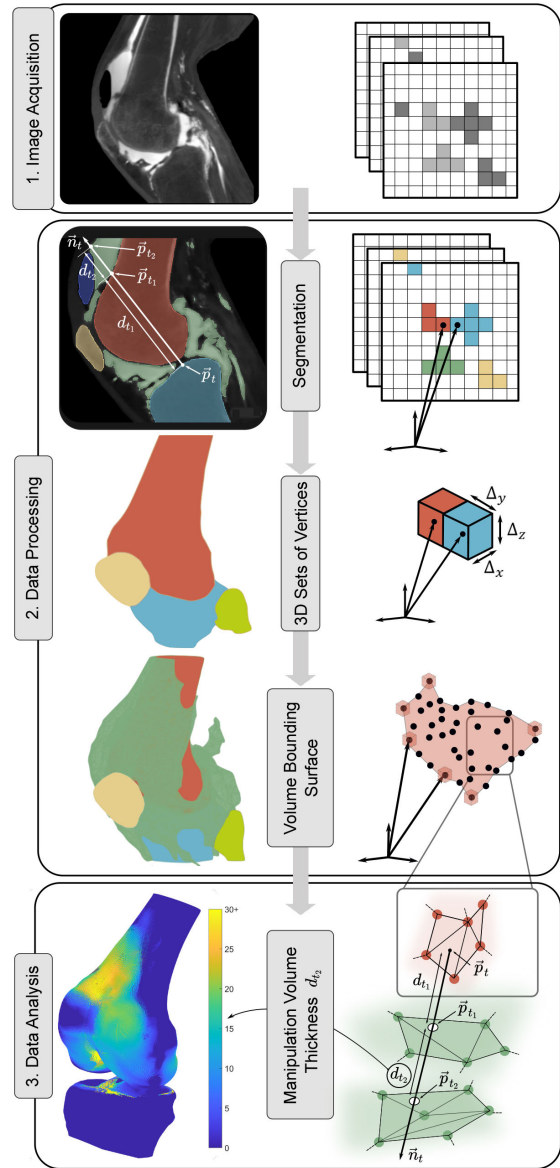


Fig. 4. Evaluation of the knee joint volume in three steps: 1. Image acquisition of the knee with the injected contrast solution using computed tomography. 2. Data processing. The bony structures and the injected volume were segmented and used to generate three-dimensional sets of vertices and their volume bounding surfaces. 3. Data analysis. Calculation of the thickness of the manipulation volume $d_{t_2}$ inside the knee joint orthogonal to the femoral and tibial bone surfaces. For each bone face, the two intersection points $\{\vec{p}_{t_1}, \vec{p}_{t_2}\}$ of the bone surface normal $\vec{n}_t$, originating from the face center point $\vec{p}_t$, with the surface of the manipulation volume were calculated. The distance between the two intersection points $d_{t_2}$ represents the thickness of the available manipulation volume above the bone surface and is visualized with a color map on the bone surface. The calculation of the distance between the bone surface and the first intersection point $d_{t_1}$ was necessary to avoid assigning nonadjacent volume to a surface point as illustrated in the segmentation picture.

femur. However, it was carried out analogously for the tibia as well.

The femur surface was represented by a triangular mesh. As a basis for the thickness calculation, the geometric center point $\vec{p}_t$ and surface normal $\vec{n}_t$ were calculated for each of the faces. In a next step, the intersection points between the femur surface
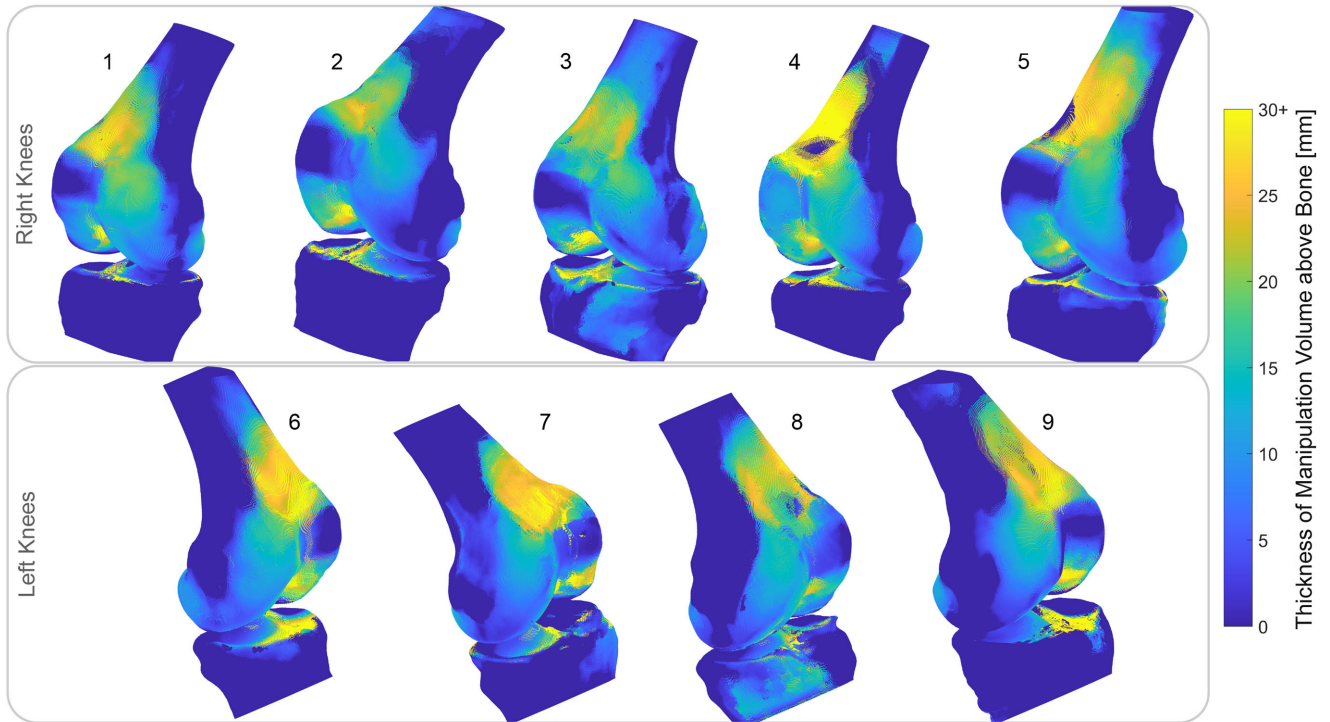
Fig. 5. Thickness of the manipulation volume inside the knee joint orthogonal to the femur and tibia surface $d_{t_2}$ for the nine examined knees. At locations where the distance $d_{t_1}$ between the bone surface and the available manipulation volume was above the threshold of 6 mm, the thickness $d_{t_2}$ was set to zero to avoid false assignments. All knees are oriented such that the medial compartment is well visible. The nine data sets and a Matlab script to generate the three-dimensional visualization according to this figure are available on the with hyperlink to https://ieee-dataport.org/open-access/manipulation-volume-inside-knee-joint-capsule.

normal $\vec{n}_t$ and the surface of the free volume inside the knee joint were computed for each face center point $\vec{p}_t$ on the femur surface (Fig. 4). Since the free volume is a closed volume, this procedure resulted in two intersection points; $\vec{p}_{t_1}$ on the surface closer to the femur, and $\vec{p}_{t_2}$ on the surface farther away from the femur. The distance $d_{t_1}$ between the face center point $\vec{p}_t$ on the femur surface and the first intersection point $\vec{p}_{t_1}$ as well as the distance $d_{t_2}$ between the first intersection point $\vec{p}_{t_1}$ and the second intersection point $\vec{p}_{t_2}$, were determined according to:

$$
\begin{aligned}
d_{t_1} &= |\vec{p}_t - \vec{p}_{t_1}|, \\
d_{t_2} &= |\vec{p}_{t_1} - \vec{p}_{t_2}|.
\end{aligned}
\tag{1}
$$

More than two intersection points can occur, because the surface normal $\vec{n}_t$ might intersect with the free joint volume at several sites. However, we are only interested in the manipulation volume that is available directly above the bone surface, the distance of which is represented by $d_{t_2}$. The distance $d_{t_1}$ represents the distance between the bone surface and the bounding surface of the available manipulation volume inside the knee joint. If the distance between the bone surface and the available free volume $d_{t_1}$ was above a threshold of 6 mm, the value for $d_{t_2}$ was set to zero to avoid assigning nonadjacent volume to a surface point (Fig. 4). The value of 6 mm was selected to account for articular cartilage between the bone surface and the manipulation volume, which was not segmented in the CT images. The thickness of the articular cartilage on the femur and tibia is in most cases below 6 mm [39]–[41].

TABLE II
DIFFERENCE BETWEEN INJECTED AND CALCULATED AMOUNT OF CONTRAST SOLUTION

| Knee | Injected [ml] | Calculated [ml] | Difference [ml] |
|---|---|---|---|
| 1 | 95 | 106 | +11 |
| 2 | 115 | 119 | + 4 |
| 3 | 115 | 153 | +36 |
| 4 | 115 | 148 | +33 |
| 5 | 115 | 132 | +17 |
| 6 | 115 | 117 | + 2 |
| 7 | 115 | 134 | +19 |
| 8 | 115 | 118 | + 3 |
| 9 | 115 | 139 | +24 |

The femur's and tibia's maximal spatial dimensions, both mediolaterally and anteroposteriorly, were assessed to provide information on the size of the different knees. For the tibia, the values were determined by measuring the bone's maximal spatial dimension in the direction of a line on a plane parallel to the transverse cutting plane and perpendicular (mediolaterally) or parallel (anteroposteriorly) to the intersection line between the transverse and the sagittal cutting planes. For the femur, the values were determined by measuring the bone's maximal spatial dimensions in the direction of a line on a plane parallel to the distal cutting plane and parallel (mediolaterally) or perpendicular (anteroposteriorly) to the intersection line between the distal and the chamfer cutting planes. The respective values were determined for several parallel planes with a distance of 1 mm to find the maximal spatial expansions.

## C. Results

The comparison of the segmented contrast solution volume with the injected contrast solution volume for all nine knees is shown in Table II. For four knees, the difference between these two volumes was below 15 ml. For the other knees, the difference was higher and up to 36 ml.

The calculated thickness of the available manipulation volume inside the knee joint capsule orthogonal to each surface point on the femur and tibia for the nine examined knees is visualized in Fig. 5.

Metrics about the size of the examined knee joints are provided in Table III. The values correspond to the maximal spatial expansion of the bones mediolaterally and anteroposteriorly. For the tibia, the spatial extension was measured in its intersection with a plane parallel to the transverse cutting plane and for the femur in its intersection with a plane parallel to the distal cutting plane.

## III. DEFINING A CUTTING WORKFLOW FOR MINIMALLY INVASIVE UKA

### A. Rationale

Based on the acquired quantitative volume inside the knee joint capsule (Section II), we aim to i) propose a cutting workflow for minimally invasive robot-assisted UKA with a laser osteotome, and ii) estimate the maximal thickness feasible for the tip of such a robotic laser osteotome. For this purpose, we need to know the thickness of the manipulation volume above the anatomical locations that need to be reached by the robotic laser osteotome to resect the bone. In a first step, we envision implanting standard UKA implants with the new, laser-based approach and thus we focused on the required bone cuts for such a standard implant. We used the obtained information on the manipulation volume inside the knee joint capsule to evaluate the thickness of this volume at the specific anatomical locations that need to be reached by the laser-cutting instrument for the implantation of a standard UKA implant (Section III-B).

Based on these results, we proposed a possible workflow for minimally invasive UKA (Section III-C) and deducted the feasible thickness of a corresponding laser-cutting tool (Section III-D).

### B. Manipulation Volume above Cutting Lines

*1) Methods:* We assumed that the endoscope tip would be positioned approximately parallel to the bone surface to minimize the required space (Fig. 1). The laser beam will enter the endoscope tip by an optical fiber. Inside the endoscope tip, the laser beam is redirected parallel to the cutting planes by the laser optics.

Three-dimensional computer-aided design models of medial femoral and tibial Aesculap univation X implants (Aesculap AG, Tuttlingen, Germany) were positioned with respect to the nine segmented knees to define the required cutting lines on the knees. The positioning of the implants was carried out by an engineer according to instructions from an orthopedic surgeon. The orthopedic surgeon approved the final implant placement. Since medial unicompartmental knee arthroplasties are performed far

### TABLE III
SIZE OF THE INVESTIGATED KNEES

| Knee | Body height [cm] | Femur size [mm] | | Tibia size [mm] | |
|---|---|---|---|---|---|
| | | med-lat* | ant-post** | med-lat* | ant-post** |
| 1 | 151 | 76 | 58 | 69 | 49 |
| 2 | 175 | 85 | 65 | 78 | 55 |
| 3 | 154 | 82 | 58 | 77 | 54 |
| 4 | 160 | 78 | 58 | 70 | 49 |
| 5 | 173 | 89 | 69 | 81 | 57 |
| 6 | 154 | 77 | 64 | 70 | 49 |
| 7 | 152 | 79 | 60 | 74 | 50 |
| 8 | 170 | 80 | 62 | 75 | 53 |
| 9 | 177 | 84 | 62 | 79 | 60 |

* maximal spatial expansion of the bone mediolaterally.
** maximal spatial expansion of the bone anteroposteriorly.

more commonly, (90-95%) [42], the focus of this paper is also kept on medial UKA.

The cutting lines are defined by the intersection of the femur or tibia surface with the implant cutting planes. These cutting planes, representing the three femoral (distal, chamfer, and posterior) and two tibial (sagittal and transverse) cuts, were derived from the corresponding implant models. Calculating the intersection between these cutting planes and the femoral surface resulted in three closed cutting lines around the femoral condyle representing the distal, chamfer, and posterior cut. The procedure resulted in two cutting lines for the tibia, the sagittal cut and the transverse cut, both with an approximately semi-circular shape. An instrument that is guided along the cutting lines requires manipulation volume also next to the cutting lines. Therefore, we were interested in the thickness of the available manipulation volume above an area on the bone surface around the cutting lines. This area was defined as the area between two lines that are equidistant to the cutting line, projected onto the bone surface. These area-bounding lines were generated with a spacing of 5 mm from the cutting line. For better comparison between the nine knees, a start, end, and middle point were defined for each cutting line (Fig. 6).

Since the envisioned laser tool should cut through the bone similar to a saw, it is not always necessary to move along the entire cutting line to cut off the bone fragment. For the closed femoral cuts, it is sufficient to move along approximately 50% of the cutting line. In contrast, for the open tibial cuts, moving along the whole cutting line might be necessary. There are many possibilities to select the cutting line segment that the instrument has to be moved along to cut off the bone fragment. These possibilities are further influenced by the angular deflections that the laser instrument can realize.

We were interested in the thickness of the available manipulation volume above the region of interest along the cutting line. Thus, the first quartile $q_1^{RoI}$, the median $m^{RoI}$, and the third quartile $q_3^{RoI}$ of the thickness of the available manipulation volume above the cutting line were calculated over the line inside the region of interest (RoI) orthogonal to the current direction of the cutting line (Fig. 7).

*2) Results:* The first quartile, as well as the median and the third quartile of the distribution of the thickness $d_{t_2}$ (Eq. (1)) of the available manipulation volume inside the knee joint capsule
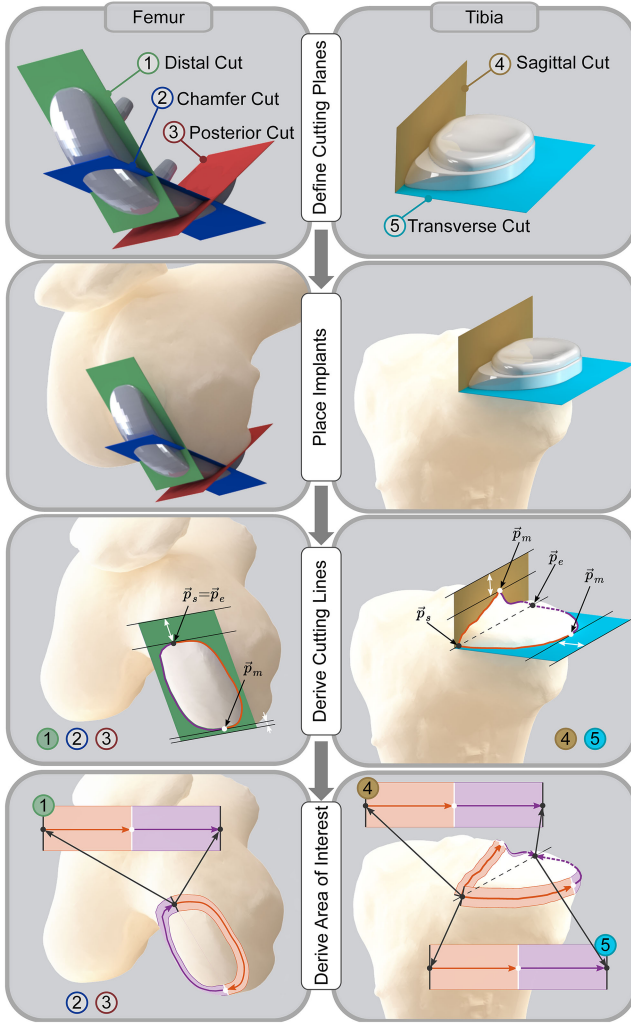
Fig. 6. Required cuts for unicompartmental knee arthroplasty, visualized for an Aesculap univation X implant. As for most unicompartmental implants, three femoral (distal, posterior, and chamfer) and two tibial (sagittal and transverse) cuts are required. For each of the nine knees, the femoral and tibial implants were placed on the medial compartment. Based on the implant planes, each cut's cutting lines were derived with respect to each bone. For each cutting line, a start point $\vec{p}_s$, middle point $\vec{p}_m$, and endpoint $\vec{p}_e$ were defined. For the femoral cuts, $\vec{p}_s = \vec{p}_e$ and $\vec{p}_m$ were defined as the points that are closest to the edge of the corresponding implant plane. For the tibial cuts, the start and endpoints were placed posterior and anterior at the bone surface points where the sagittal and transverse implant planes intersect. The middle points $\vec{p}_m$ were defined as the points farthest from the intersection line of the sagittal and transverse implant planes. The region of interest on the bone surface along the cutting lines was defined as the area between two equidistant lines to the cutting line. The calculated thickness of the available manipulation volume above this bone area inside the knee joint capsule was analyzed.

over the points inside the region of interest, orthogonal to the cutting lines for all required cuts are shown in Fig. 8.

## C. Proposed Workflow for Minimally Invasive UKA

*1) Methods:* Based on visual inspection of the distribution of the available manipulation volume along the cutting lines
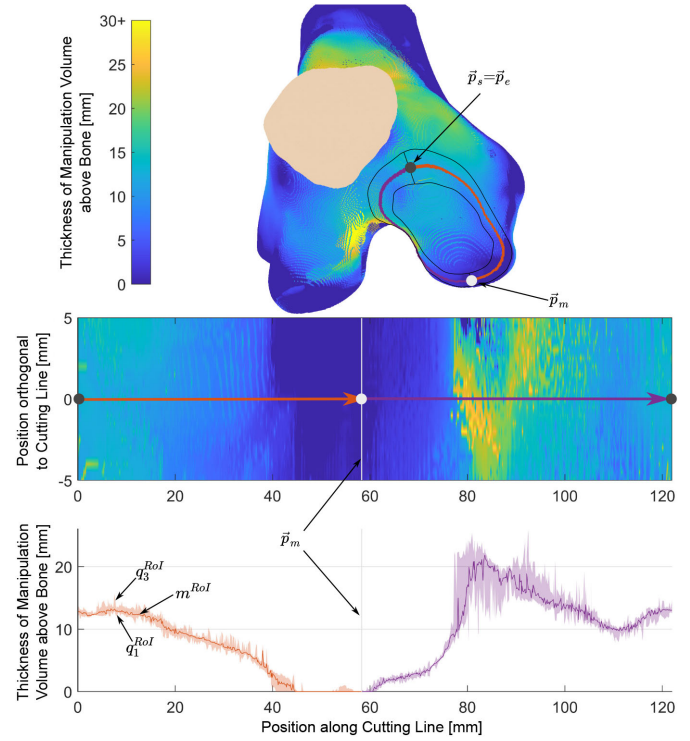


Fig. 7. Analysis of the thickness of the available manipulation volume along an area around the cutting line, shown exemplarily for the distal cut on the femoral condyle. The thickness of the available manipulation volume was extracted for an area on the bone surface around the cutting line. The first quartile $q_1^{RoI}$, the median $m^{RoI}$, and the third quartile $q_3^{RoI}$ were calculated for each position along the cutting line over 20 points inside the region of interest (RoI), orthogonal to the cutting line.

(Fig. 8), we deduced a possible workflow for minimally invasive UKA using a robotic laser osteotome that should provide maximal space for tool manipulation.

*2) Results:* We made the following observations for the femoral cuts: Along the distal cutting line, the thickness of the free manipulation volume above the bone surface was higher in the intercondylar region of the femur (Fig. 8, violet lines) than on the outer side (orange lines), and higher at the anterior end ($\{\vec{p}_s, \vec{p}_e\}$) than at the posterior end of the condyle (grey area). For the posterior cut, there was more manipulation volume at the proximal part (grey area) than at the distal part ($\{\vec{p}_s, \vec{p}_e\}$) of the cut. In case of the tibia, we made the following observations: There was very little to no manipulation volume available for most knees along the entire transverse cutting line and the first and last portion of the sagittal cutting line. Therefore, we conclude that the cutting locations to perform the transverse cut and parts of the sagittal cut are, in most cases, not directly accessible for a robotic instrument without prior tissue preparation, such as lifting off the knee joint capsule to provide access to the bone surface. This was expected because this preparation step is also often performed in conventional UKA before cutting.

Based on these observations, we propose the following workflow: First, the distal cut could be performed by moving the instrument along the cutting line mainly on the intercondylar region of the femur ($[0 - 14\%, 64 - 100\%]$). Second, the
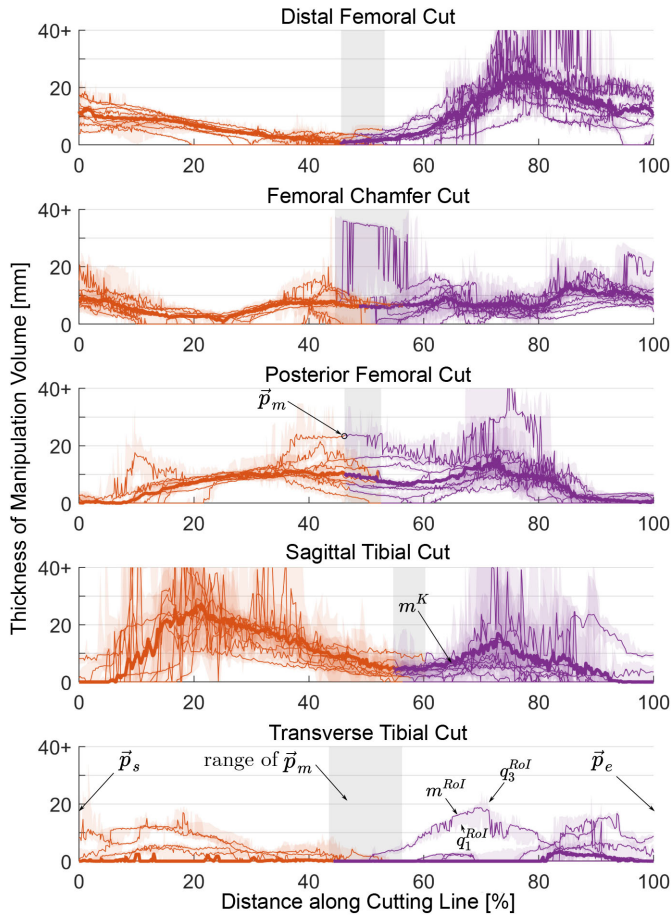
Fig. 8. The thickness of the available manipulation volume inside the knee joint capsule for the nine examined knees: The first quartile $q_1^{RoI}$, the median $m^{RoI}$, and the third quartile $q_3^{RoI}$ of the manipulation volume thickness $d_{t_2}$ distribution over the region of interest (RoI) perpendicular to the cutting line on the femur and tibia surface are plotted along the cutting line with a threshold of 6 mm for $d_{t_1}$ for each knee. The orange and violet-colored items mark the cutting lines between the start point $\vec{p}_s$ and the middle point $\vec{p}_m$ and between the middle point $\vec{p}_m$ and the end point $\vec{p}_e$, respectively. The bold line indicates the median thickness of all nine knees $m^K$. The grey areas represent the range of $\vec{p}_m$ for all nine knees. This figure is available as supplementary material with a different color coding that maps the lines to the corresponding knee number.

chamfer cut could be performed either by moving the instrument mainly along the intercondylar region of the femur ($[0 - 5\%, 55 - 100\%]$), or from the distal cutting surface taking advantage of the additional space that will be available as soon as the bone fragment from the distal cut is removed. Third, the posterior cut could be performed either by moving the instrument along the proximal part of the cutting line ($[24 - 74\%]$), or from the chamfer cutting surface taking advantage of the additional space that will be available as soon as the bone fragment from the chamfer cut is removed. In case the second options are chosen for the chamfer and posterior cut, the instrument would have to allow for a higher laser deflection angle. For the sagittal cut, we see mainly two options. Either the instrument could be moved along the entire length of the sagittal cutting line, locally cutting the tibia from proximal to distal, or the instrument could be moved along the anterior part of the tibia from distal to proximal, locally

cutting the bone from anterior to posterior. However, the first and last parts of the sagittal cut might not be directly accessible for a robotic instrument without prior tissue preparation. Similarly, the transverse cut seems to be inaccessible for a robotic instrument without prior tissue preparation.

### D. Feasible Tool Dimensions

*1) Methods:* Due to the variability of the manipulation volume thickness and its distribution inside the knee joint it is not straightforward to draw a general quantitative conclusion on the feasible instrument size. Therefore, we calculated the first quartile and the median of the available manipulation volume's thickness above the region of interest along the proposed portions of the femoral cutting lines (Section III-C) for all knees.

*2) Results:* The first quartile $q_1^{RoI}$ and the median $m^{RoI}$ of the available manipulation volume thickness above the region of interest along at least 50% of each femoral cutting line for all knees were; distal: 9.1 mm, 13.3 mm, chamfer: 4.9 mm, 7.6 mm, and posterior: 6.6 mm, 9.6 mm. Based on these results, we assume that an instrument thickness of $5 - 8$ mm would be feasible for the proposed procedure. The feasible instrument dimensions for the tibial cuts will depend on the tissue preparation procedure.

## IV. DISCUSSION

We analyzed the thickness of the available manipulation volume inside the knee joint above the femur and tibia surface by injecting contrast solution and performing CT scans. This is the first time that quantitative information on the three-dimensional distribution of the maximally available volume inside the knee joint was determined to the best of our knowledge. This information is crucial when developing minimally invasive robotic tools for knee surgery that introduce substantial changes into existing surgical workflows and for applications that critically depend on knowledge about the available manipulation volume inside the knee.

The amount of injected contrast solution was 95 ml or 115 ml. However, the calculated volume of the contrast solution inside the knee joint after injection varied between 106 ml and 153 ml, i.e., it was always bigger than the injected volume. The amount of synovial fluid in a normal human knee joint has been reported to be less than 4 ml [43], thus the presence of synovial fluid is unlikely to explain the discrepancy. We assume that the difference originates from the fact that we used Thiel-embalmed bodies and that the fixation fluid present inside the knee joint mixed with the contrast solution.

The manipulation volume was not distributed evenly around the knee joint, but the general distribution of the injected contrast solution was similar for all nine examined knees (Fig. 5). For all knees, there was little to no manipulation volume below the patella (fat pad), below the medial and lateral collateral ligaments, and on the medial side of the medial tibial condyle. Locations with most manipulation volume included the recessus suprapatellaris and the anterior intercondylar area. The recessus suprapatellaris is a bulge of the knee capsule. Therefore, the available volume inside the recessus suprapatellaris does not

directly connect to the bone surface and is not a valid manipulation volume for interventions that require access to the bone surface. It was not possible to avoid this false assignment by setting a threshold for $d_{t_1}$ because the recessus suprapatellaris is very thin and may lie directly on the bone surface. An area with less manipulation volume is visible in the supratrochlear region for knees 4 and 8. This effect could be caused by the plica suprapatellaris, an inward fold of the knee joint capsule, which increases the distance between the bone surface and the volume inside the recessus suprapatellaris $d_{t_1}$ above the threshold of 6 mm.

To extract quantitative information on the available manipulation volume for UKA, we examined the available manipulation volume at the locations relevant for this procedure, i.e., the cutting lines that need to be reached by a surgical instrument to perform bone cutting with a laser for placing a standard medial UKA implant (Fig. 8). The thickness of the available manipulation volume changes along the cutting lines due to the different anatomical locations and corresponding different environmental conditions along the cutting lines, i.e., the presence and flexibility of the soft tissue at each location. The differences in the thickness of the manipulation volume between the different subjects were mainly caused by anatomical differences, e.g., the different form, consistency, and elastic properties of soft tissue inside the knee joint. Noticeable higher median values or variability of the manipulation volume thickness for individual knees were mainly caused by either leakage of the contrast solution or a local connection of the manipulation volume between the two knee compartments (e.g., between 65% and 80% of the posterior cutting line, or between 40% and 60% of the chamfer cutting line in Fig. 8). The selected embalming technique (Thiel) is known to preserve the tissue's natural consistency but increases its softness and permeability [44]. We assume that the observed contrast solution leakages were mainly caused by the softer tissue due to the Thiel-embalming and/or the presence of Baker's cysts.

Based on this study's results, we proposed a workflow for minimally invasive UKA, which should be feasible with a robotic laser osteotome with a thickness of $5 - 8$ mm. Our conclusions apply only for guiding the instrument along the femoral cutting lines. Further experiments with prior tissue preparation to provide access to the bone surface (lifting off the knee joint capsule) would be necessary to propose a feasible surgical workflow for the tibial cuts. We only investigated the required space to perform the cuts, but not how the instrument is inserted into the knee or moved between the cuts. Thus, the complete workflow might impose further limitations on the maximal tool size.

We did not specifically analyze the limitations on the width and length of the tool because the shape of the tool is still undefined. Instead, we specified a region of interest around the cutting lines with a width of 10 mm. This area considers that a surgical tool has a certain width and, therefore, also requires manipulation space on both sides of the cutting line. Depending on the specific shape of the tool, the relevant volume around the cutting lines might differ. However, we assume that the tool's width and length will have similar dimensions to allow the tool's rotation inside the knee joint. Also, we assume that the required manipulation volume depends on the shape of the cut and the

tool's length. Depending on the tool's length, more manipulation volume might be required at locations where a cutting line has a high curvature, and the instrument is required to change direction within little space.

We proposed that the distal and chamfer cuts could be performed by moving the instrument mainly along the femur's intercondylar region. The anterior and posterior cruciate ligaments attach to the intercondylar areas between the medial and the lateral condyle. Since Thiel-embalming increases tissue permeability [44], we cannot exclude that the soft tissue present in the knee, such as the cruciate ligaments or the infrapatellar fat pad, was partially infiltrated by contrast solution and that therefore parts of these anatomical structures were considered as manipulation volume. This entails that, in reality, less manipulation volume might be present in the intracondylar region than suggested by our results. Therefore, performing the chamfer/posterior cuts from the distal/chamfer cutting surfaces, taking advantage of the additional space available as soon as the bone fragment from the distal/chamfer cuts are removed, might be preferable.

Due to the limited number of knees studied in this work and the different tissue properties of dead tissue compared to living tissue, our results might not directly apply to the target population for UKA. In addition, the knees studied originated from elderly people. Therefore, this study's results might not directly represent the situation in the knee of a younger person. For instance, anatomical structures such as cruciate ligaments or menisci might be altered due to the aging process or injuries, or osteophytes might obstruct space that is normally available.

The accuracy of the data is further limited due to the limited resolution of the CT images and the segmentation process. Assuming an inaccuracy of the segmentation in the range of 2-3 pixels, the segmentation error should be less than 1 mm.

Furthermore, this study only considered one type of standard implant. Different implant shapes will result in different cutting lines on the femur and tibia and, therefore, influence the resulting available manipulation volume around the cutting lines.

The presented procedure allows evaluating the available manipulation space inside a joint on an individual basis. Therefore, we also see the possibility that this method might be used in a clinical setting in the future to allow for personalized interventions. The data can serve as a valuable information basis for personalized implant designs, surgical instruments, trajectory planning, or the optimal selection of the surgical access points to the joint. Additional limitations might apply if this method is used in a clinical setting. First, radiation exposure should be minimized, i.e., it should be considered to use MRI instead of CT. Second, the segmentation should be carried out automatically to reduce duration and costs. However, most importantly, the personalized procedure needs to show a clear benefit for the patient to justify the additional costs and potential risks, e.g., infections or hematoma due to the incision of liquid into the joint.

This study was carried out at one fixed knee flexion angle. We assume that it is beneficial for robotic minimally invasive surgery in the knee to carry out the procedure with a static knee flexion angle. Changing the knee flexion angle might allow increasing the manipulation volume at specific locations but would most

likely require to retract and reinsert the robotic instrument. It has been shown that the relationship between the volume and pressure inside the knee joint capsule depends on the flexion angle of the knee [45]. The capsular pressure seems to be higher in a flexed knee than an extended knee, leading to a higher risk of high intraarticular pressure and capsular rupture. Therefore, should the method presented in this paper be used in patients or healthy subjects, the capsule's maximal feasible pressure should be identified and not exceeded to avoid ruptures of the capsule. Furthermore, it could be valuable to investigate the change of the available manipulation volume's distribution depending on the knee flexion angle. This would require to change the experimental procedure and setup to include an outlet that allows the contrast solution to flow out of the knee joint if necessary.

The herein presented method to measure the manipulation volume was based on a uniform pressure distribution in the entire knee joint capsule. In contrast, the robotic tool's insertion will not introduce a uniform pressure distribution in the knee but only extend the capsule volume and pressure locally. Thus, we do not expect to reach problematic intraarticular pressures during the procedure. Given that the soft tissue has sufficient elasticity, the available manipulation volume might be bigger in a surgical setting than what we found in this study because fluid is inserted into the knee capsule with little to no pressure in a surgical setting.

Despite the mentioned limitations, the obtained quantitative information on the amount and distribution of the thickness of the manipulation volume inside the knee joint indicates that using a $5-8$ mm robotic laser osteotome for UKA seems reasonable. After the first design of this tool, further analysis of the volume data will allow assessing the entire procedure's feasibility by also considering the instrument manipulation in between the different cuts and considering the specific shape of the entire instrument.

## V. Conclusion

We presented a method to quantitatively evaluate the available volume inside a joint to manipulate surgical instruments. We implemented this method for Thiel-embalmed knee specimen and derived quantitative information on the available manipulation volume size and distribution. We observed a similar but uneven distribution of the volume around the knee joint for the nine examined knees. To derive requirements for minimally invasive UKA, we analyzed the manipulation volume at the specific locations that a surgical tool needs to reach to perform minimally invasive bone cutting to place a medial implant in UKA. This analysis made it possible to propose a surgical workflow for minimally invasive UKA that provides a large volume for manipulation of the tool, such as a flexible robotic laser osteotome. Based on the findings we derived that a tool thickness of $5-8$ mm could be feasible to perform the femoral cuts. A further preparation step will be necessary prior to the tibial cuts, to provide access to the bone surface.

The presented method and the resulting quantitative information on the available manipulation volume can serve as a basis for the development of robotic tools for minimally invasive knee surgery that introduce significant changes in an existing surgical workflow, the design of novel implants, the optimization of surgical workflows, and, in the future, even for personalized interventions.

## References

[1] K. Yang *et al.*, "Minimally invasive unicondylar versus total condylar knee arthroplasty-early results of a matched-pair comparison," *Singap. Med. J.*, vol. 44, no. 11, pp. 559–562, 2003.

[2] P.-F. Sun and Y.-H. Jia, "Mobile bearing UKA compared to fixed bearing TKA: A randomized prospective study," *The Knee*, vol. 19, no. 2, pp. 103–106, 2012.

[3] S. Bengtson and K. Knutson, "The infected knee arthroplasty: A 6-year follow-up of 357 cases," *Acta Orthopaedica Scandinavica*, vol. 62, no. 4, pp. 301–311, 1991.

[4] M. S. Noticewala *et al.*, "Unicompartmental knee arthroplasty relieves pain and improves function more than total knee arthroplasty," *The J. Arthroplasty*, vol. 27, no. 8, pp. 99–105, 2012.

[5] C. T. Laurencin *et al.*, "Unicompartmental versus total knee arthroplasty in the same patient. a comparative study," *Clin. Orthopaedics Related Res.*, no. 273, pp. 151–156, 1991.

[6] J. Newman *et al.*, "Unicompartmental or total knee replacement: The 15-year results of a prospective randomised controlled trial," *J. Bone Joint Surg., Brit. volume*, vol. 91, no. 1, pp. 52–57, 2009.

[7] O. Robertsson *et al.*, "Use of unicompartmental instead of tricompartmental prostheses for unicompartmental arthrosis in the knee is a cost-effective alternative: 15,437 primary tricompartmental prostheses were compared with 10,624 primary medial or lateral unicompartmental prostheses," *Acta Orthopaedica Scandinavica*, vol. 70, no. 2, pp. 170–175, 1999.

[8] J. Plate *et al.*, "Unicompartmental knee arthroplasty: Past, present, future," *Reconstructive Rev.*, vol. 2, no. 1, 2012.

[9] W. G. Hamilton *et al.*, "Incidence and reasons for reoperation after minimally invasive unicompartmental knee arthroplasty," *J. Arthroplasty*, vol. 21, no. 6, pp. 98–107, 2006.

[10] J. N. Weinstein *et al.*, "Factors influencing walking and stairclimbing following unicompartmental knee arthroplasty," *J. Arthroplasty*, vol. 1, no. 2, pp. 109–115, 1986.

[11] J. P. McAuley *et al.*, "Revision of failed unicompartmental knee arthroplasty," *Clin. Orthopaedics Related Res.*, vol. 392, pp. 279–282, 2001.

[12] P. E. Müller *et al.*, "Influence of minimally invasive surgery on implant positioning and the functional outcome for medial unicompartmental knee arthroplasty," *J. Arthroplasty*, vol. 19, no. 3, pp. 296–301, 2004.

[13] A. D. Pearle *et al.*, "Robot-assisted unicompartmental knee arthroplasty," *J. Arthroplasty*, vol. 25, no. 2, pp. 230–237, 2010.

[14] M. Roche *et al.*, "Robotic arm-assisted unicompartmental knee arthroplasty: Preoperative planning and surgical technique," *Amer. J. Orthoped. (Belle Mead, NJ)*, vol. 38, no. Suppl. 2, pp. 10–15, 2009.

[15] J. H. Lonner *et al.*, "Robotic arm-assisted uka improves tibial component alignment: A pilot study," *Clin. Orthopaedics Related Res.*, vol. 468, no. 1, p. 141, 2010.

[16] A. Battenberg *et al.*, "Robotic-assisted unicompartmental knee arthroplasty," in *Partial Knee Arthroplasty*. Springer, 2019, pp. 123–132.

[17] J. P. van der List *et al.*, "Robotic-assisted knee arthroplasty: An overview," *Amer. J. Orthoped.*, vol. 45, no. 4, pp. 202–211, 2016.

[18] R. N. De Steiger *et al.*, "Computer navigation for total knee arthroplasty reduces revision rate for patients less than sixty-five years of age," *J. Bone Joint Surg.*, vol. 97, no. 8, pp. 635–642, 2015.

[19] M. A. Conditt and M. W. Roche, "Minimally invasive robotic-arm-guided unicompartmental knee arthroplasty," *J. Bone Joint Surg.*, vol. 91, no. Suppl. 1, pp. 63–68, 2009.

[20] B. Wei *et al.*, "Laparoscopic versus open appendectomy for acute appendicitis: A metaanalysis," *Surg. Endoscopy*, vol. 25, no. 4, pp. 1199–1208, 2011.

[21] B. de Goede *et al.*, "Meta-analysis of laparoscopic versus open cholecystectomy for patients with liver cirrhosis and symptomatic cholecystolithiasis," *Brit. J. Surg.*, vol. 100, no. 2, pp. 209–216, 2013.

[22] M. Eugster *et al.*, "Positioning and stabilization of a minimally invasive laser osteotome," in *Proc. Hamlyn Symp. Med. Robot.*, vol. 10, 2017, pp. 21–22.

[23] J. Burgner, "Robot assisted laser osteotomy," Ph.D. dissertation, Karlsruher Inst. für Technologie, Karlsruhe, Germany, 2010.

[24] A. Fuchs *et al.*, "Fast and automatic depth control of iterative bone ablation based on optical coherence tomography data," in *Proc. Eur. Conf. Biomed. Opt.* Optical Society of America, 2015, p. 95420P.

[25] M. Augello *et al.*, "Comparative microstructural analysis of bone osteotomies after cutting by computer-assisted robot-guided laser osteotome and piezoelectric osteotome: An in vivo animal study," *Lasers Med. Sci.*, vol. 33, no. 7, pp. 1471–1478, 2018.

[26] M. Eugster *et al.*, "Accuracy evaluation of a novel parallel robot for minimally invasive laser osteotomy," *Submitted for Publication.*

[27] M. Eugster *et al.*, "Design evaluation of a stabilized, walking endoscope tip," in *Int. Workshop Med. Serv. Robots.* Springer, 2020, pp. 127–135.

[28] N. Simaan *et al.*, "Medical technologies and challenges of robot-assisted minimally invasive intervention and diagnostics," *Annu. Rev. Control, Robot., Auton. Syst.*, vol. 1, pp. 465–490, 2018.

[29] R. Reilink *et al.*, "Image-based flexible endoscope steering," in *Proc. IEEE/RSJ Int. Conf. Intell. Robots Syst.*, 2010, pp. 2339–2344.

[30] J. Ruiter *et al.*, "Design and evaluation of robotic steering of a flexible endoscope," in *Proc. 4th IEEE RAS EMBS Int. Conf. Biomed. Robot. Biomechatronics (BioRob)*, 2012, pp. 761–767.

[31] M. C. Cavusoglu *et al.*, "Workspace analysis of robotic manipulators for a teleoperated suturing task," in *Proc. IEEE/RSJ Int. Conf. Intell. Robots Syst. Expanding Societal Role Robot. Next Millennium*, vol. 4, 2001, pp. 2234–2239.

[32] H. Visser *et al.*, "Forces and displacements in colon surgery," *Surg. Endoscopy*, vol. 16, no. 10, pp. 14 263–1430, 2002.

[33] L. Capek *et al.*, "The analysis of forces needed for the suturing of elliptical skin wounds," *Med. Biol. Eng. Comput.*, vol. 50, no. 2, pp. 193–198, 2012.

[34] M. Eugster *et al.*, "Contact force estimation for minimally invasive robot-assisted laser osteotomy in the human knee," in *Joint Workshop New Technol. Comput./Robot Assist. Surg.*, vol. 8, 2018.

[35] P. J. McNair *et al.*, "Swelling of the knee joint: Effects of exercise on quadriceps muscle strength," *Arch. Phys. Med. Rehabil.*, vol. 77, no. 9, pp. 896–899, 1996.

[36] M. Benkhadra *et al.*, "Flexibility of thiel's embalmed cadavers: The explanation is probably in the muscles," *Surg. Radiologic Anatomy*, vol. 33, no. 4, pp. 365–368, 2011.

[37] 3D Slicer. [Online]. Available: https://www.slicer.org/

[38] S. Pieper *et al.*, "3D Slicer," in *Proc. 2nd IEEE Int. Symp. Biomed. Imag.: Nano Macro*, 2004, pp. 632–635.

[39] G. Ateshian *et al.*, "Quantitation of articular surface topography and cartilage thickness in knee joints using stereophotogrammetry," *J. Biomech.*, vol. 24, no. 8, pp. 761–776, 1991.

[40] Z. A. Cohen *et al.*, "Knee cartilage topography, thickness, and contact areas from mri: In-vitro calibration and in-vivo measurements," *Osteoarthritis Cartilage*, vol. 7, no. 1, pp. 95–109, 1999.

[41] D. Shepherd and B. Seedhom, "Thickness of human articular cartilage in joints of the lower limb," *Ann. Rheumatic Dis.*, vol. 58, no. 1, pp. 27–34, 1999.

[42] J. R. Smith *et al.*, "Fixed bearing lateral unicompartmental knee arthroplasty–short to midterm survivorship and knee scores for 101 prostheses," *The Knee*, vol. 21, no. 4, pp. 843–847, 2014.

[43] M. W. Ropes *et al.*, "The origin and nature of normal human synovial fluid," *J. Clin. Investigation*, vol. 19, no. 6, pp. 795–799, 1940.

[44] H.-J. Wilke *et al.*, "Thiel-fixation preserves the non-linear load–deformation characteristic of spinal motion segments, but increases their flexibility," *J. Mech. Behav. Biomed. Materials*, vol. 4, no. 8, pp. 2133–2137, 2011.

[45] D. A. Funk *et al.*, "Effect of flexion angle on the pressure-volume of the human knee," *Arthroscopy: J. Arthroscopic Related Surg.*, vol. 7, no. 1, pp. 86–90, 1991.